https://doi.org/10.5194/egusphere-2024-3147
Preprint. Discussion started: 17 October 2024

Impacts of Sea Ice Leads on Sea Salt Aerosols and Atmospheric Chemistry in the Arctic

Erin J. Emme[1,*]; Hannah M. Horowitz[1,2,*]

[1]Department of Civil and Environmental Engineering, University of Illinois Urbana-Champaign, Urbana, Illinois, USA

[2]Department of Atmospheric Science, University of Illinois Urbana-Champaign, Urbana, Illinois, USA

*Corresponding authors: Erin J. Emme, emme2@illinois.edu, and Hannah M. Horowitz, hmhorow@illinois.edu.

https://doi.org/10.5194/egusphere-2024-3147
Preprint. Discussion started: 17 October 2024

Impacts of Sea Ice Leads on Sea Salt Aerosols and Atmospheric Chemistry in the Arctic

Erin J. Emme[1], Hannah M. Horowitz[1,2]

[1]Department of Civil and Environmental Engineering, University of Illinois at Urbana-Champaign, Urbana, 61801, USA

[2]Department of Atmospheric Sciences, University of Illinois at Urbana-Champaign, Urbana, 61801, USA

***Correspondence to*: Erin J. Emme (emme@illinois.edu) and Hannah Horowitz (hmhorow@illinois.edu)**

Abstract. Sea salt aerosols (SSA) alter Arctic climate through interactions with radiation and clouds. The processes contributing to Arctic cold season (November-April) SSA remain uncertain. Observations from coastal Alaska suggest emissions from open leads in sea ice, which are not included in climate models, may play a dominant role. Their Arctic-wide significance has not yet been quantified. Here, we combine satellite data of lead area (the AMSR-E product) and a chemical transport model (GEOS-Chem) to quantify pan-Arctic SSA emissions from leads during the cold season from 2002-2008 and predict their impacts on atmospheric chemistry. Lead emissions vary seasonally and interannually. Total monthly SSA emissions increase by 1.0-1.8% (≥60°N latitude) and 5.8-8.4% (≥75°N). The AMSR-E product detects at least 50% of total lead area as compared to optical MODIS satellite images. SSA concentrations increase primarily at the location of leads, where standard model concentrations are low. GEOS-Chem overestimates SSA concentrations at Arctic sites even when lead emissions are not included, suggesting underestimation of SSA sinks and/or uncertainties in SSA emissions from blowing snow and open leads. Multi-year monthly mean surface bromine atom (Br) concentrations increase 2.8-8.8% due to SSAs from leads. Changes in ozone concentrations are negligible. While leads contribute <10% to Arctic-wide SSA emissions in the years 2002-2008, these emissions occur in regions of low background aerosol concentrations. Leads are also expected to increase in frequency under future climate change. Thus, lead SSA emissions could have significant impacts on Arctic climate.

Short Summary

There is uncertainty in the sources of Arctic cold season (November-April) sea salt aerosols. Using a chemical transport model and satellite observations, we quantify Arctic-wide sea salt aerosol emissions from fractures in sea ice, called open sea ice leads, and their atmospheric

https://doi.org/10.5194/egusphere-2024-3147
Preprint. Discussion started: 17 October 2024

chemistry impacts for the cold season. We show sea ice leads contribute to Arctic sea salt aerosols and bromine, especially in under-observed regions.

1. Introduction

Sea salt aerosols (SSA) affect Arctic climate by scattering incoming solar radiation and acting as cloud condensation nuclei and ice nuclei (DeMott et al., 2016; Pierce and Adams, 2006; Quinn et al., 1998). Long-term measurements have shown that peak SSA concentrations in the Arctic occur during the cold season (Leaitch et al., 2018; Quinn et al., 2002; Schmale et al., 2021). However, the sources and mechanisms of cold season SSA emissions are uncertain, which hinders atmospheric chemistry and climate models from accurately representing polar regions. Recent observations from Utqiaġvik, Alaska have suggested that open leads, or open sea ice fractures, are an important source of cold season SSA emissions (Kirpes et al., 2019; May et al., 2016). Climate change has impacted the Arctic by rapidly decreasing sea ice age and thickness (Intergovernmental Panel On Climate Change, 2023; Sumata et al., 2023; Vaughan et al., 2013), and future projections indicate this will continue (Intergovernmental Panel On Climate Change, 2023), suggesting the amount of open leads will increase in the future due to thinner ice that is prone to fracture. More work is needed to discern the Arctic-wide importance and impacts of SSA emissions from sea ice leads ("lead emissions") on atmospheric chemistry and climate. By combining satellite observations and chemical transport modeling, we quantify the significance and impacts of lead emissions on atmospheric concentrations of SSA and bromine and evaluate simulated SSA against in-situ observations.

Several observational studies have investigated the importance of lead-based SSA. Key observations in the 1970s in Utqiaġvik, Alaska, by Scott & Levin (1972) and Radke et al. (1976) demonstrated an increase in sodium-containing particles in the presence of open water leads. More recently, a multi-year study of observed SSA at Utqiaġvik (May et al., 2016), conducted over all seasons, found that leads are a significant contributor to SSA through wind-driven production; Nilsson et al. (2001) estimate that leads contribute an order of magnitude less than the open ocean to the Arctic SSA flux during the summer months. Held et al. (2011) found that leads do not contribute significantly to Arctic summertime SSA under low wind speeds below the threshold for open sea spray aerosol production (~4 m s^{-1}). Kirpes et al. (2019) identified SSA produced by local leads as the dominant aerosol source in the coastal Alaskan Arctic during winter months. In addition, Willis et al. (2018) suggest that lead emissions are more important in winter and early

https://doi.org/10.5194/egusphere-2024-3147
Preprint. Discussion started: 17 October 2024

spring as winds over the Northern oceans are at their highest. Chen et al. (2022) also shows in a recent study during the month of April at Utqiaġvik, that leads were present locally throughout the study, and that they contributed to sea spray aerosol production. As ground-based observations in the Arctic are mainly limited to coastal stations, it is difficult to estimate the significance and impacts of lead emissions over the entire Arctic. Representing Arctic-wide emissions from leads in a global chemical transport model, especially during the cold season, will help discern whether lead emissions and their impacts on atmospheric chemistry are significant enough to warrant inclusion in chemistry as well as climate models.

Other modeling studies in the Arctic and observations primarily from Antarctica suggest blowing snow, where saline snow over sea ice is swept up by wind, is a potential major contributor of cold season SSA in polar regions. In two chemical transport models, the inclusion of additional SSA emissions from blowing snow brought simulated SSA mass concentrations closer to what was observed (Confer et al., 2023; Huang et al., 2018; Huang and Jaeglé, 2017; Rhodes et al., 2017). Other potential sources of cold season SSA, such as frost flowers, have been found to be insignificant (Alvarez-Aviles et al., 2008; Roscoe et al., 2011; Yang et al., 2017). Incorporating blowing snow SSA emissions into models has shown how missing sources of SSA in the Arctic can have a significant impact on atmospheric chemistry (Huang et al., 2020), emphasizing the need to assess the potential impacts of lead emissions, which are currently missing from global chemistry and climate models. One study incorporates SSA emissions from leads in a chemical transport model (WRF-Chem), but the study was limited to the 400 km^2 area surrounding Utqiaġvik, Alaska and used ERA-5 reanalysis sea ice fraction to define the presence of leads (Ioannidis et al., 2022). They find open leads are the primary source of fresh and aged SSA in Utqiaġvik, Alaska during the cold season, consistent with the observational analysis by May et al. (2016) and Kirpes et al. (2019).

SSA play a critical role in Arctic tropospheric chemistry. SSA debromination is the main global source of reactive bromine in the troposphere (Wang et al., 2021). Reactive bromine chemistry has been attributed to the rapid depletion of ozone in the Arctic springtime, which reaches a maximum in March-April (Simpson et al., 2007). In particular, bromine atom (Br) is key to these ozone depletion events; it is produced through the photolysis of Br_2, which is sourced from SSA debromination and snowpack chemistry (Abbatt et al., 2012; Dibb et al., 2010; Pratt et al., 2013; Stutz et al., 2011). Swanson et al. (2022) show improved springtime model-observation agreement of BrO by including a snowpack photochemistry mechanism based on multiple field

https://doi.org/10.5194/egusphere-2024-3147
Preprint. Discussion started: 17 October 2024

observations in a global chemical transport model. While on a global scale, reaction of OH with other SSA-sourced bromine species can also produce Br (Wang et al., 2021), this is minor in polar regions due to low OH concentrations. Br rapidly depletes ozone through heterogeneous reactions, which produce BrO that can photolyze to reform Br, creating a catalytic ozone-depletion cycle (Simpson et al., 2007).

Here, we estimate the pan-Arctic contribution of leads to total SSA emissions during the cold season for the years 2002-2008, by using satellite observations of lead area to parameterize lead-based SSA production in the global chemical transport model GEOS-Chem. We evaluate simulated SSA concentrations against observations and predict the impacts of lead SSA emissions on atmospheric chemistry, including concentrations of Br and ozone.

2. Methods

2.1 Satellite Data of Lead Area Fractions

In this study, we use satellite data of lead area fractions to inform the GEOS-Chem chemical transport model (next section) of where leads are present. The Advanced Microwave Scanning Radiometer-Earth Observation System (AMSR-E) sensor aboard NASA's Aqua satellite records brightness temperatures from Earth at six different frequencies (https://www.cen.uni-hamburg.de/en/icdc/data/cryosphere/lead-area-fraction-amsre.html) (Integrated Climate Data Center (ICDC) et al., n.d.), which are converted to lead area fractions following the algorithm of Röhrs and Kaleschke (2012). This method of detection can only be applied to the Arctic freezing season (November-April) due to surface melt of the sea ice May-October. Daily data is available at 6.25 km horizontal resolution, as the algorithm is not limited by cloud cover. For the rare individual days with missing data in the dataset (0.8%), we use the average lead area fraction for that month. The lead area fraction includes open water leads and thin ice-covered leads 3 km and wider. The data spans latitudes 41° to 90°N, though a majority of Arctic sea ice lies above 60°N and leads are therefore unlikely to be present at lower latitudes.

We choose the AMSR-E product for this study as it avoids cloud interference and provides nearly consistent daily resolution. Röhrs and Kaleschke (2012) qualitatively validated this lead dataset against the Moderate Resolution Image Spectroradiometer (MODIS) and found that more than 50% of the total lead area visible in 500 m MODIS images was detected. However, the MODIS

https://doi.org/10.5194/egusphere-2024-3147
Preprint. Discussion started: 17 October 2024

sea surface temperature product is constrained to clear-sky conditions, with Arctic winter conditions affecting cloud identification techniques (Hoffman et al., 2022); it is also difficult to discern the thermal contrast and shape of cloud edges and shadows from the temperature contrast of leads (Reiser et al., 2020).

2.2 GEOS-Chem: global chemical transport model

Here we use the 3-D atmospheric transport model GEOS-Chem (geos-chem.org) version 13.2.1 https://doi.org/10.5281/zenodo.5500717 (Community, 2021). Within GEOS-Chem, the Harmonized Emissions Component (HEMCO) computes emissions for different sources, regions, and species (Keller et al., 2014). GEOS-Chem and HEMCO are driven by Modern-Era Retrospective Analysis for Research and Applications (MERRA-2) (Gelaro et al., 2017) meteorological fields from NASA Global Modeling and Assimilation Office (GMAO).

SSA emissions calculations for the open ocean use a wind (Gong, 2003; Monahan et al., 1986)- and sea surface temperature-dependent (Jaeglé et al., 2011) source function. In polar regions, SSA emissions from blowing snow are also included (Huang and Jaeglé, 2017). SSA have two size bins: coarse mode (SALC; r= 0.5 to 10 μm) and accumulation mode (SALA; r= 0.1 to 0.5 μm). For gas and aerosol species, wet deposition includes washout and rainout in convective and large-scale stratiform precipitation (Amos et al., 2012; Liu et al., 2001; Wang et al., 2014). Dry deposition of gas and aerosol species follows a resistance-in-series approach, and includes gravitational settling of sea salt (Jaeglé et al., 2011; Pound et al., 2020; Wang et al., 1998; Zhang et al., 2001). Coupled gas- and multiphase-reactive halogen chemistry, including sea salt debromination, acid displacement, and photolysis and oxidation of gas-phase inorganic bromine and chlorine species, is described in Wang et al. (2021). This version of GEOS-Chem does not include snowpack chemistry as a source of reactive bromine in the standard model. We parameterize SSA emissions from leads with the same function as the open ocean emissions from Jaegle et al. (2011) (Eq. (S.1) in the Supplemental Information (SI)), scaled by the fractional area of leads in each grid cell from the AMSR-E satellite data. The AMSR-E satellite data is regridded to 0.5°x0.625° from 6.25x6.25 km using a distance-weighted average remapping. This is a unique wind- and SST-dependent source function for calculating lead emissions, driven by satellite observations defining the presence of leads. Nilsson et al. (2001) derive an empirical lead emissions flux with an exponential dependence on windspeed and no consideration of SST (Eq. (S.2) in SI), and for a given windspeed find lower emissions from than the open ocean due to a

https://doi.org/10.5194/egusphere-2024-3147
Preprint. Discussion started: 17 October 2024

lower fetch. Ioannidis et al. (2022) use a similar source function to this study which has slight differences in the exact SST and wind speed dependencies compared to GEOS-Chem; emissions from leads follow the same function as the open ocean and they define the presence of leads as the fraction of each grid cell which is ice-free. Figure 1 shows an example of the daily temporal frequency and spatial resolution of the AMSR-E satellite data (both the raw (a) and regridded (b)) used to drive the model.

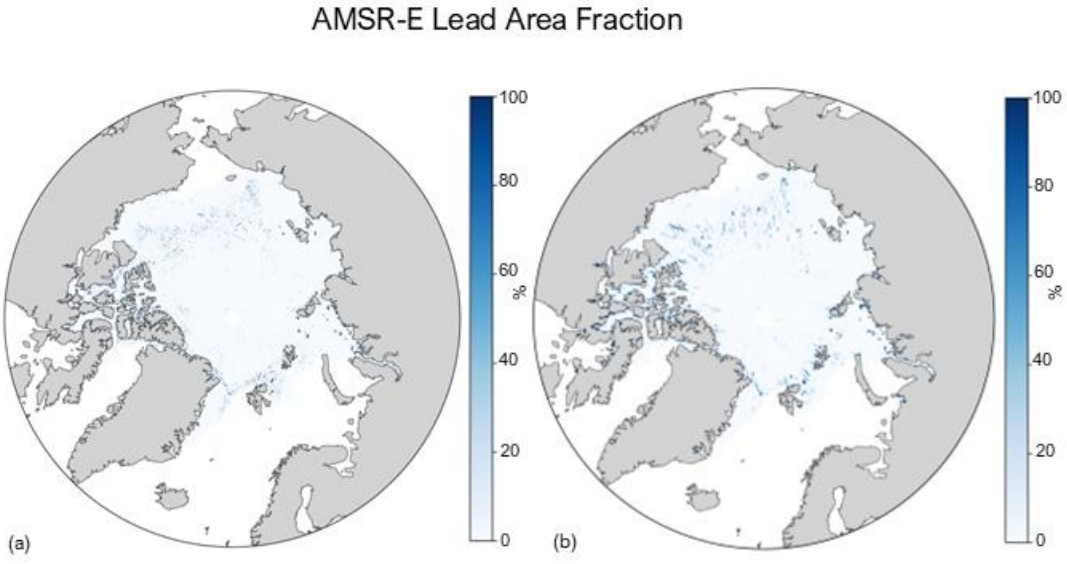

Figure 1- Map of AMSR-E daily lead area fraction in percent (%) for November 1, 2002, both raw (6.25-km resolution) (a) and re-gridded (0.5˚x0.625˚ resolution) (b).

We perform simulations to quantify lead emissions and their impact on atmospheric chemistry at the highest global horizontal (2° latitude x 2.5° longitude) and vertical (72 vertical levels) resolution. We first calculate SSA emissions at the highest resolution of HEMCO (0.5°x0.625°), which is the native resolution of MERRA-2. Emissions are then implemented into GEOS-Chem "offline" to ensure total SSA emissions are properly scaled and not influenced by the resolution-dependence of the wind speed (Lin et al., 2021). We calculate two sets of emissions for two simulations: (1) the standard emissions only (i.e., open ocean and blowing snow SSA emissions, the "standard" case); (2) SSA emissions with lead emissions added ("standard + leads" case). The absolute difference between the two is the SSA emissions from leads, and we present the percent change due to leads (%) as calculated with Eq. (1).

https://doi.org/10.5194/egusphere-2024-3147
Preprint. Discussion started: 17 October 2024

$$Percent\ change\ due\ to\ leads\ (\%) = \frac{(Standard+leads)_{simulation} - (Standard)_{simulation}}{(Standard)_{simulation}} \times 100 \quad (1)$$

Simulations are performed for the years 2002-2008, when there is overlap between the AMSR-E satellite data and available observed Arctic SSA concentrations at multiple sites, following one year of initialization. Because satellite observations of lead area fractions begin November 1, 2002, we initialize the standard + leads case for GEOS-Chem with standard + leads SSA emissions for one year (November 1, 2002 to November 1, 2003) and then start the simulation for analysis on November 1, 2002, with the spun-up November 1, 2003, initial conditions. For the standard case, the initialization year begins November 1, 2001. For both cases, we simulate SSA concentrations, evaluate against observed concentrations, and assess the impacts of additional lead emissions on atmospheric chemistry. This includes analysis of the change in atmospheric concentrations of bromine atom (Br) and ozone (O_3). For model evaluation, GEOS-Chem does not track sodium (Na^+) content for SSA, so we convert simulated SSA to Na^+ mass concentrations using a factor of $\frac{1}{3.256}$, which is based on the mass ratio of Na^+ in seawater (Confer et al., 2023; Huang and Jaeglé, 2017; Riley and Chester, 1971).

2.3 In-Situ Observations of Arctic Sea Salt Aerosol Concentrations

We evaluate simulated concentrations of SSA from GEOS-Chem, converted to Na^+ concentrations, against in situ observations of Na^+ concentrations at 3 Arctic sampling sites: Utqiaġvik, Alaska (71.3°N, 156.6°W; 11m a.s.l.) (Quinn et al., 2002); Zeppelin Mountain, Svalbard, Norway (78.9°N, 11.9°E; 475m a.s.l.) (World Meteorological Organization (WMO), 2003); Alert, Nunavut, Canada (82.5°N, 62.5°W; 210m a.s.l.) (World Meteorological Organization (WMO), 2003). In winter months, these coastal sites border mostly ice-covered ocean (Huang and Jaeglé, 2017). At Utqiaġvik, mass concentrations of Na^+ for submicron and supermicron aerosols are separated, while the other two sites measure the total mass concentration without size distinction. The Na^+ mass concentrations are determined from ion chromatography with uncertainties of 5-11%, or an absolute uncertainty of 0.01 μg/m^3 (Quinn et al., 2000; World Meteorological Organization (WMO), 2003). The aerosol sampling frequency is daily at Zeppelin and Utqiaġvik (submicron) and weekly at Alert and Utqiaġvik (supermicron).

3. **Results**

https://doi.org/10.5194/egusphere-2024-3147
Preprint. Discussion started: 17 October 2024

242

243 *3.1 Emissions of Sea Salt Aerosols from Leads*

244

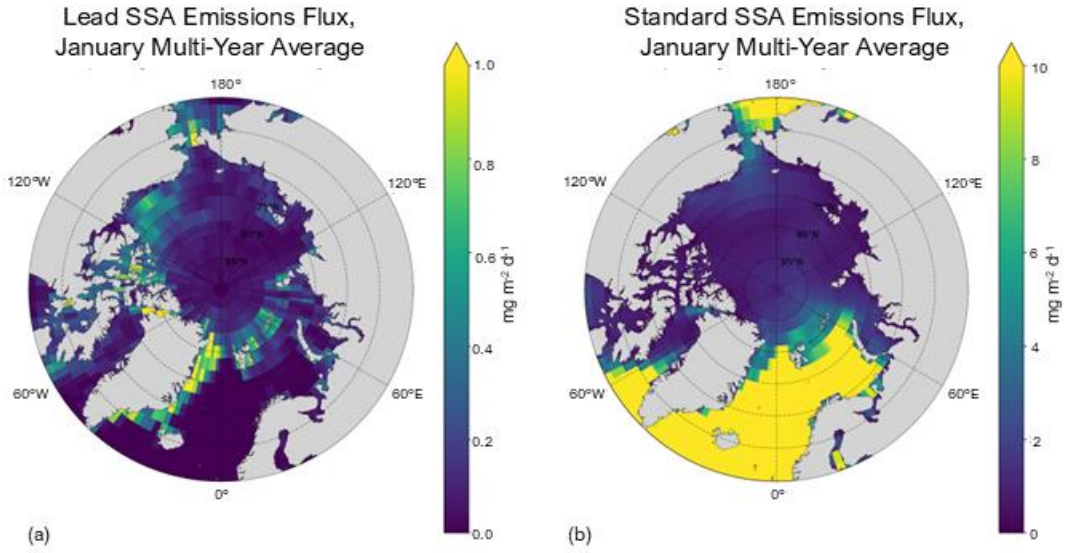

245

246 **Figure 2-** Total (coarse + accumulation mode) lead SSA emissions (a) and standard SSA
247 emissions (b), averaged over 2002-2008 for January. Note the difference in magnitude of the
248 colorbar of (a) and (b).

249

250 Figure 2a shows the spatial distribution of multi-year (2002-2008) average lead emissions for the
251 month of January, which is a climatology based on model simulations that use daily resolution
252 lead data (e.g., Fig. 1). We focus Figs. 2 and 4 on the month of January as it is the month with
253 the highest relative increase in SSA emissions for latitudes 75°N and higher (Table 1). Alongside
254 Fig. 2a is the standard model, which includes open ocean and blowing snow emissions (Fig. 2b;
255 see Sect. 2.2). Total emissions are resolution independent and are shown in Fig. 2 for the
256 2.0°x2.5° resolution of the online atmospheric chemistry simulation. We find the lead emissions
257 are concentrated in regions where leads are present and occur in regions where the standard
258 SSA emissions are low (e.g., in the Greenland Sea and parts of the Barents Sea). The percent
259 change in SSA emissions due to leads (calculated with Eq. (1)) is detailed in Table 1 and Fig. 2;
260 Figs. 4, 5, and S.4 show the percent change in SSA concentration due to leads. Generally,
261 emissions tend to be higher from 70° to 80° N and more concentrated off the coasts of Northern
262 Canada and Greenland, as opposed to off the coast of Northern Russia and Europe. Month to

https://doi.org/10.5194/egusphere-2024-3147
Preprint. Discussion started: 17 October 2024

month, regions where emissions are higher remains similar while the magnitude varies (see Fig. S.1 in SI).

Month	Multi-Year (2002-2008) Average Monthly Percent Change in SSA Emissions due to Leads	
	≥60°N	≥75°N
November	1.1% ± 0.18%	7.6% ± 2.4%
December	1.3% ± 0.26%	7.6% ± 2.5%
January	1.4% ± 0.19%	8.4% ± 4.2%
February	1.6% ± 0.32%	7.5% ± 2.2%
March	1.7% ± 0.19%	7.3% ± 1.7%
April	1.8% ± 0.20%	5.8% ± 1.5%

Table 1- Monthly average percent change in SSA emissions due to leads (calculated using Eq. (1)) ±1 standard deviation, averaged for 2002-2008, for ≥60°N and ≥75°N.

Table 1 shows the percent change in multi-year monthly average SSA emissions due to leads for 60° to 90°N latitude (≥60°N) and 75° to 90°N (≥75°N**)**. Leads are more important to total SSA emissions at higher latitudes due to large open ocean emissions in the North Atlantic at lower latitudes (see Fig. 2b) and the spatial variability of the lead emissions (Fig. 2a). The percent increase due to leads is ~4-6% higher for ≥75˚ N than for ≥60˚ N latitude. The month with the highest contribution to SSA emissions from leads varies with the region being analyzed. Poleward of 75°N, SSA emissions increase most from leads in January, whereas poleward of 60°N, emissions increase most in April. As shown from the standard deviations in Table 1, there is interannual variability in the percent increases.

https://doi.org/10.5194/egusphere-2024-3147
Preprint. Discussion started: 17 October 2024

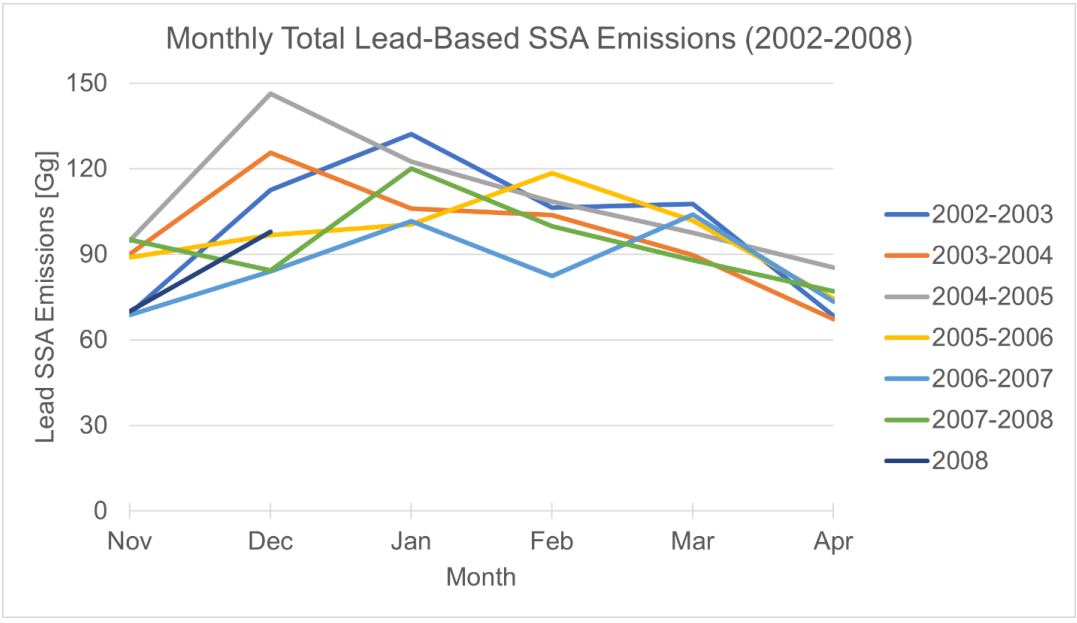

Figure 3- Monthly variations of total (coarse + accumulation mode) lead emissions of SSA during the cold season for 2002-2008. Each line includes November and December of the first year and January through April of the following year, except for the year 2008, which only includes November and December of 2008.

We find that the magnitude of lead emissions varies by month and year, as well as seasonally (see Fig. 3 and Figs. S.1 and S.2). Monthly total lead emissions and lead area have low correlation (R^2= 0.13, see Fig. S.3), indicating the variance in monthly total lead emissions is dominated by the nonlinear dependencies on wind speed and sea surface temperature (see Sect. 2.2). In most years, lead emissions decrease from January-April, but there is no single month when lead emissions peak each year (Fig. 3). There is also no clear interannual trend in cold season total lead emissions (see Fig. S.2). Lead emissions are lowest in the 2006-2007 cold season and highest in the 2004-2005 cold season (Fig. S.2). We find that the annual total lead area in the Arctic over the full period of the AMSR-E satellite data (2002-2011) has statistically significantly increased (see Fig. S.4 (b) and Text S.2 in the SI). Based on satellite observations of leads using methods of detection such as AMSR-2 and thermal-infrared satellite imagery, it is unclear if there is a significant observable trend in Arctic lead area from 2011 to the present (Li et al., 2022; Reiser et al., 2020; Wang et al., 2016), especially due to cloud interference with lead detection (Hoffman et al., 2022). However, climate models consistently predict Arctic sea ice will continue to thin (high confidence) and the presence of first year sea ice vs. multi-year sea ice will increase (very high

https://doi.org/10.5194/egusphere-2024-3147
Preprint. Discussion started: 17 October 2024

confidence) (Intergovernmental Panel On Climate Change, 2023). This suggests there could be an increasing trend in lead area in the future, which would increase lead emissions.

3.2 Atmospheric Chemistry Impacts of Sea Ice Leads

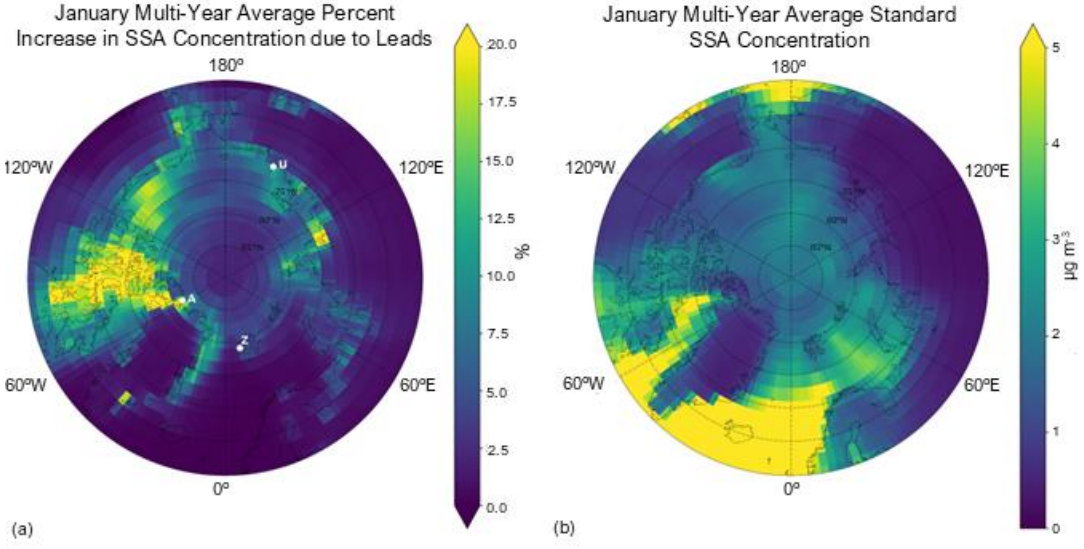

Figure 4- Percent change due to leads (calculated with Eq. (1)) in SSA mass concentration (a) and the standard surface SSA mass concentration in μg m^{-3} (b) for the January multi-year (2002-2008) average. White points in (a) represent the respective locations of each observational site: Alert, Nunavut, Canada (A); Utqiaġvik, Alaska (U); Zeppelin Mountain, Svalbard, Norway (Z).

Figure 4a shows the spatial distribution of the multi-year (2002-2008) average percent change due to leads in surface SSA mass concentration, alongside the standard simulated SSA mass concentration (Fig. 4b) for the month of January. With the addition of leads, the average Arctic-wide (≥60°N) percent increase in multi-year mean January SSA mass concentrations is 3.3%, and the maximum percent increase in an individual model gridbox is 60.5%. We find that the greatest percent increases due to leads in SSA mass concentrations occur at the location of lead emissions (see Fig. 2a), where the standard concentrations are also very low, except off the eastern coast of Greenland, where the percent increase is reduced due to the high background SSA concentrations in the Greenland Sea (Fig. 4b) from open ocean emissions (Fig. 2b).

https://doi.org/10.5194/egusphere-2024-3147
Preprint. Discussion started: 17 October 2024

Figure 5a shows the average Arctic-wide percent increase due leads in multi-year monthly mean SSA mass concentration for each cold season month. Averaged poleward of 60°N, the percent increase due to leads in SSA mass concentration remains relatively constant throughout the cold season, but there is a slight decreasing trend from November-April when averaged poleward of 75°N (Fig. 5a). Changes in SSA mass concentration are also higher poleward of 75°N. However, the percent increase in SSA mass concentration for both latitudinal ranges have large spatial variability, as seen in the standard deviation in Fig. 5a. The spatial distribution of the percent increase in SSA mass concentration due to leads remains similar month to month (see Fig. S.5 in SI).

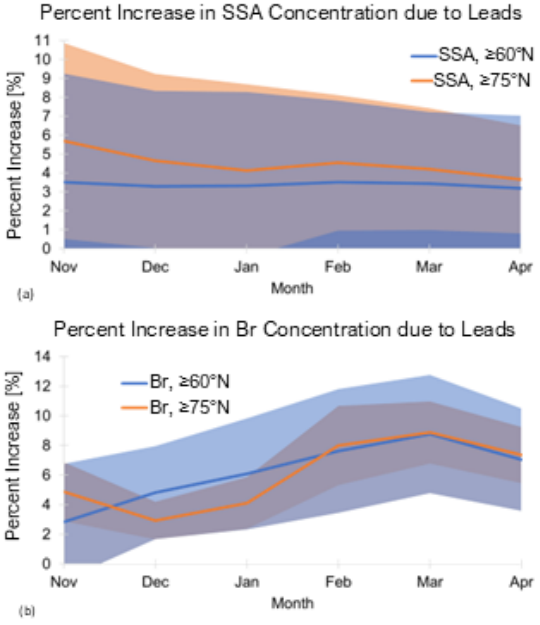

Figure 5. Multi-year (2002-2008) monthly mean percent increase due leads (calculated with Eq. (1)) in surface (a) SSA and (b) Br concentrations averaged across different Arctic regions (blue line: ≥60˚ N; orange line: ≥75˚ N). Shaded area represents ±1 standard deviation.

As described in Sect. 1, SSA contribute to the production of tropospheric reactive bromine and thereby bromine atom (Br). Here we examine changes in Br due to its role in ozone depletion events.

https://doi.org/10.5194/egusphere-2024-3147
Preprint. Discussion started: 17 October 2024

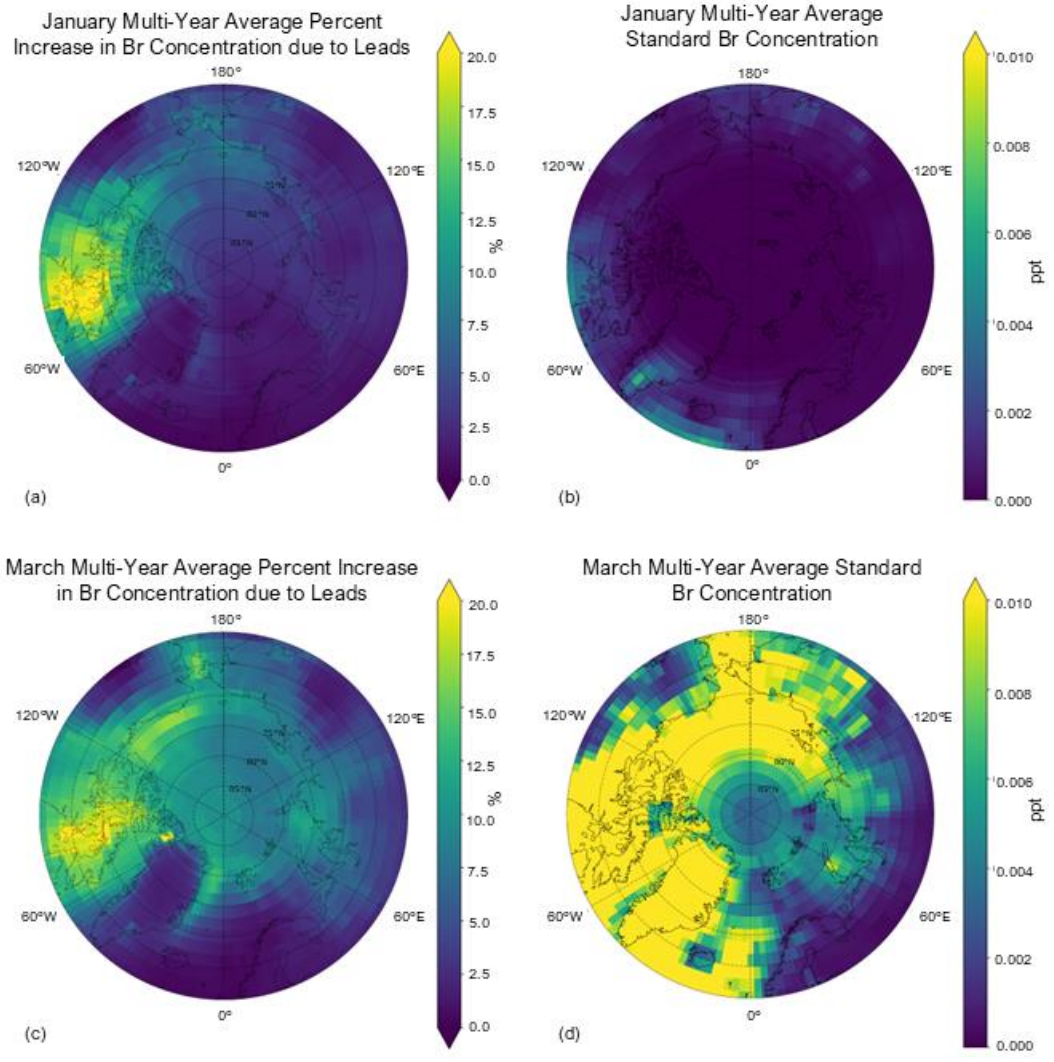

Figure 6- Multi-year (2002-2008) mean January (a and b) and March (c and d) percent increase due to leads in surface Br concentration (a and c) and the standard model surface Br concentration in ppt (b and d).

Figure 6 shows the multi-year (2002-2008) mean percent increase due to leads in surface Br concentrations and the standard Br concentration (in parts per trillion, or ppt) for the month of January (Fig. 6a and 6b) and March (Fig. 6c and 6d), respectively. Increased SSA from leads increases surface levels of Br across all months during the cold season (Fig. 6a and 6c, Fig. S.7 in the SI for other months). These increased concentrations spatially follow the increased SSA

https://doi.org/10.5194/egusphere-2024-3147
Preprint. Discussion started: 17 October 2024

mass concentrations from leads (Fig. 4a) with differences due to where Br can be produced photochemically from the precursors released from SSA. The spatial distribution of increased Br from leads remains relatively similar month to month during the cold season. However, the changes in Br concentration in February to April occur over a larger area (Fig. 6c and Fig. S.7), likely due to the seasonality of Arctic bromine chemistry, which is influenced by increasing area where sunlight is available to photolyze Br-sourced SSA species. The average Arctic-wide (≥60°N) percent increase due to leads in multi-year January mean surface Br concentration is 6.1% and the maximum increase in an individual gridbox is 35%; for March, it is 8.8% and 20.4%, respectively. Overall, the average monthly percent increase in Br concentration is higher than the corresponding increases in SSA concentration, particularly after January, and reaches a maximum in March (see Fig. 5). The percent change due to leads in Br concentrations increases from November-March poleward of 60°N and from December-March poleward of 75°N (Fig. 5b). This does not strictly follow the seasonality of lead emissions (Fig. 3) or the percent increase in SSA concentrations due to leads (Fig. 5a), likely due to more available sunlight for photochemical reactions that produce Br later in the cold season. Increases in surface Br concentration could lead to decreased surface ozone concentrations. We find that the percent decrease due to leads in average surface ozone concentrations during the Arctic cold season, however, are negligible (< -0.25%).

3.3 Evaluation Against Sea Salt Aerosol Observations

We compare modeled and observed sodium (Na^+) mass concentrations at three long-term monitoring stations to evaluate the performance of the simulation with and without additional lead emissions. The locations of each observational site are shown in Fig. 4a.

https://doi.org/10.5194/egusphere-2024-3147
Preprint. Discussion started: 17 October 2024

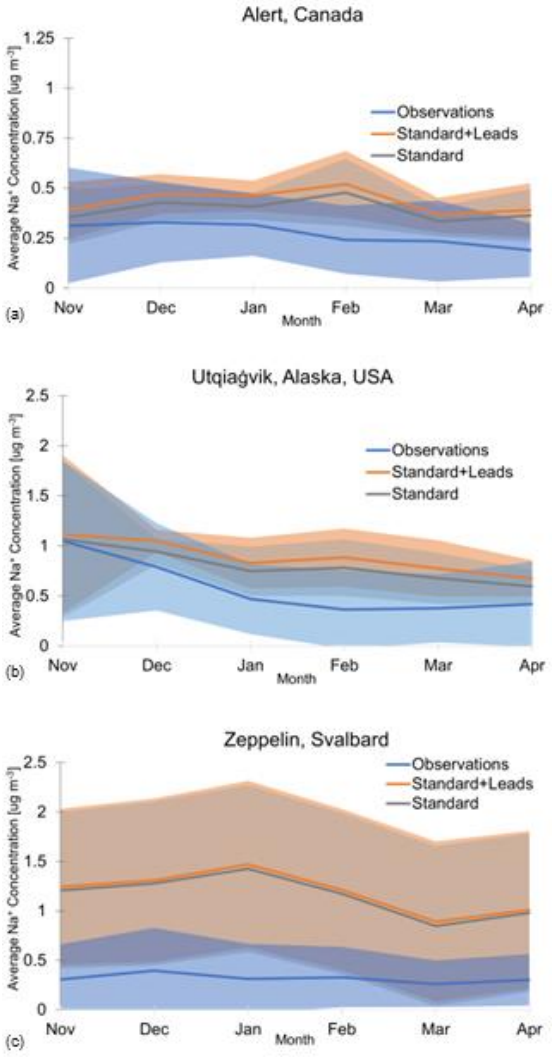

Figure 7- Observed (blue line) and simulated (gray and orange lines) multi-year monthly mean sodium mass concentrations at (a) Alert, Canada, (b) Utqiaġvik, Alaska, and (c) Zeppelin, Norway for the cold seasons of 2002-2008. Shaded regions are ±1 standard deviation. Note the y-axis for Alert (a) is half as large as Utqiaġvik (b) and Zeppelin (c).

Figure 7 shows multi-year (2002-2008) monthly mean Na^+ concentrations in the observations (blue), standard + leads simulation (orange), and standard simulation (grey) for Alert (7a), Utqiaġvik (7b), and Zeppelin (7c) during the cold season. We sample the model simulations in the gridbox that encompasses the latitude, longitude, and altitude of each monitoring station (see

https://doi.org/10.5194/egusphere-2024-3147
Preprint. Discussion started: 17 October 2024

Sect. 2.3) and convert the simulated SSA to Na^+ concentrations. For all sites and months during the cold season, the simulated and observed Na^+ mass concentrations overlap within ± 1 standard deviation (shaded regions in Fig. 7). We find mean concentrations are overpredicted in both the standard and standard + leads simulations at all sites and months during the cold season, apart from the standard model at Utqiaġvik and Alert in November which agree closest with observations.

The model overpredicts Na^+ concentrations the most at Zeppelin, with the standard + leads and standard mean concentrations a factor of 3.35 to 4.71 higher than observations across all months during the cold season. Confer et al. (2023) similarly find an overprediction of SSA at Zeppelin, which they find is exacerbated by including blowing snow emissions. Additionally, Zeppelin is at high elevation (located on a mountain at 475m) and has been found to be more impacted by the free troposphere and aerosol-cloud interactions than other Arctic sites (Freud et al., 2017); the chemical transport model cannot represent two-way aerosol-cloud interactions. The model overestimate is less at Utqiaġvik, where the standard + leads simulation still overpredicts observed concentrations by a factor of 1.06 to 2.43, and least at Alert, with observed concentrations overestimated by a factor of 1.18 to 2.15 for the standard + leads model. Lead emissions do not change the simulated seasonality of cold season surface SSA concentrations. The timing of cold season maximum and minimum concentrations at Alert and Zeppelin differs between the observed and simulated, for both the standard + leads and standard models. At Utqiaġvik, the maximum mass concentration in the observations and both model simulations occurs in November. However, the minimum observed cold season mass concentration occurs in February at Utqiaġvik, whereas the standard + leads and standard mean concentrations reach a minimum in April.

Figure 4a places the differences seen at each of the three sites in Fig. 7 into broader context, with a map of the relative increase in SSA mass concentrations for the month of January. The most significant relative increase in SSA concentration from leads out of the three sites occurs at Alert (Fig. 7a). However, regions with the highest percent increases in SSA mass concentration due to leads in Fig. 4a for the month of January (i.e., parts of Northern Canada southwest of Alert), which are consistent throughout the cold season (Fig. S.4 in SI), are not sampled by ground monitoring sites, which would help constrain lead impacts on SSA. In our simulation, lead emissions have the same size distribution as the open ocean, with most of the mass in the coarse mode (82-90%). Despite this, there are increases in SSA concentration over land (Fig. 4a) indicating

https://doi.org/10.5194/egusphere-2024-3147
Preprint. Discussion started: 17 October 2024

transport (see also Text S.3 and Fig. S.6). This is consistent with observed inland transport of SSA across the North Slope of Alaska (Simpson et al., 2005). It is likely that leads emit smaller SSA particles relative to open ocean emissions (Nilsson et al., 2001), which would increase their lifetime, so non-local impacts from leads may be greater than simulated here. This further highlights the need for observations in other regions to better understand the impacts of lead emissions.

There is strong observational evidence that lead emissions contribute to cold season SSA (see Sect. 1), but the standard model consistently overpredicts observed SSA concentrations prior to inclusion of additional lead emissions. This suggests other sources of SSA may be overpredicted or sinks of SSA may be underpredicted. Ongoing work to improve the treatment of aerosol wet removal processes in GEOS-Chem has not specifically investigated the impacts on sea salt aerosol (Luo et al., 2020; Luo and Yu, 2023). Additionally, a recent observational study (Chen et al., 2022) suggests that the GEOS-Chem blowing snow emissions parameterization may overpredict the frequency of blowing snow events, therefore possibly contributing to the overprediction of Arctic SSA mass concentrations.

To test these possible sources of uncertainty, we run two additional sensitivity simulations for one cold season (November 2002-April 2003): (1) using the Luo et al. (2020) wet deposition scheme with the standard + leads SSA emissions ("standard + leads + Luo Wet Deposition") and (2) turning off blowing snow emissions in the standard model for an "open ocean only" case (see Text S.4 for further description). We find that the Luo wet deposition scheme improves model agreement most at Zeppelin (see Fig. S.8(c) in SI), especially in the months of November, December, and April. However, at Utqiaġvik, the Luo wet deposition scheme results in underestimates in Na^+ concentrations compared to observations (Fig. S.8(b)). At Alert, the Luo wet deposition scheme decreases the model overestimate of the standard + leads simulation when compared to the observations for the 2002-2003 cold season (Fig. S.8(a)), but still overestimates Na^+ concentrations in each month. As the 2002-2003 observations at Alert are particularly low, we also include the observed multi-year (2002-2008) monthly average Na^+ concentrations for comparison. The Luo wet deposition scheme improves model evaluation from February-March compared to the multi-year average observed concentrations at Alert, but otherwise underpredicts concentrations.

https://doi.org/10.5194/egusphere-2024-3147
Preprint. Discussion started: 17 October 2024

At Utqiaġvik, too-low Na^+ concentrations with only open ocean emissions suggest that this site is influenced by blowing snow emissions and/or lead emissions. Of the three sites, blowing snow is most important and well-represented here, as it also improves the modeled seasonality; there may be larger uncertainty in the emissions parameterization in other regions. At Zeppelin and Alert, even with open ocean emissions only and the standard wet deposition, the model overestimates Na^+ concentrations for all months during the cold season for 2002-2003. The results of these sensitivity tests suggest that changes to wet scavenging may be more important at higher altitudes, given the improvement in model evaluation at Zeppelin. Yet, the inclusion of the Luo wet deposition scheme to the standard+leads simulation still overestimates concentrations at Alert, highlighting there are remaining uncertainties associated with the scheme; Luo & Yu (2023) find that it overestimates wet scavenging on a global scale. There may be a need for improved representation of the model deposition processes to resolve SSA overestimates.

4. Conclusions

Observational evidence (Chen et al., 2022; Kirpes et al., 2019; May et al., 2016; Radke et al., 1976; Scott and Levin, 1972; Willis et al., 2018) and one modeling study of the 400 km^2 region around Utqiaġvik, Alaska (Ioannidis et al., 2022) have shown that leads may be an important source of cold season SSA for the coastal Arctic. Here, we evaluate their importance as an Arctic-wide source of cold season SSA emissions and their potential atmospheric chemistry impacts in the global chemical transport model GEOS-Chem.

We find that lead SSA emissions occur primarily in regions where other SSA emissions sources are very low, mainly within the Canadian archipelago and the eastern Greenland Sea. Poleward of 75° N, leads increase total monthly cold-season SSA emissions by 5.8 to 8.4%, with the highest contribution of SSA emissions from leads in January and the lowest in April. Lead emissions vary in magnitude by month and year, mainly due to variations in lead area. Future trends in Arctic sea ice predicted by climate models suggest a possible future increasing trend in lead area (Intergovernmental Panel On Climate Change, 2023), which would increase lead emissions. Therefore, we expect present-day and future lead emissions to be more significant than the time period analyzed in this study (years 2002-2008), which could increase atmospheric chemistry impacts. The additional SSA from leads in regions where the background aerosol concentrations are low could also affect aerosol-cloud interactions, which largely have a warming effect in the

https://doi.org/10.5194/egusphere-2024-3147
Preprint. Discussion started: 17 October 2024

Arctic from trapping of longwave radiation during the cold season (Cox et al., 2015; Stramler et al., 2011). This could potentially lead to additional climate feedbacks from expected future climate change-driven increases in sea ice lead emissions.

SSA mass concentrations increase primarily at the location of lead emissions, in regions where the standard concentration is very low (≤1.2 μg m^{-3}). Throughout the cold season, the increased SSA mass concentrations from leads remain relatively constant in magnitude and spatial distribution. The highest increase in multi-year average SSA mass concentrations due to leads, spatially averaged for ≥75°N, occurs in November (5.7%) and the lowest occurs in April (3.7%). Increased SSA from leads increases surface Br concentrations during the cold season. The percent increase due to leads in SSA and Br concentrations are spatially coherent. We find total Arctic-wide (≥60°N) increases in multi-year mean surface Br concentration range from 2.8 to 8.8%. The increases in Br are not sufficient to have an impact on ozone; subsequent decreases in average surface ozone concentrations in the Arctic are negligible (< -0.25%).

Our model evaluation reveals SSA is overestimated in the standard and standard+leads model at each of the 3 Arctic sampling sites, which points to possible sources of uncertainty. First, Nilsson et al. (2001) suggest leads emit smaller SSA particles relative to the open ocean, but only Utqiagvik provides aerosol size distinction. There are also no available ground observations where we predict the highest relative increases in SSA mass concentrations. To better constrain lead impacts on SSA and reduce uncertainty in the SSA size distribution, additional ground observations with size distribution information in the Canadian archipelago, such as off the northern coast of Baffin Island and the eastern coast of Victoria Island, would be beneficial. Next, we attempt to better understand the overprediction of SSA mass concentrations with two additional sensitivity simulations but are unable to ultimately confirm the source(s) of overprediction. Ongoing improvements in the representation of aerosol wet deposition processes could significantly impact simulated SSA mass concentrations (Luo et al., 2020; Luo and Yu, 2023). Additionally, there are uncertainties associated with blowing snow emissions and its GEOS-Chem parameterization, suggesting the need for more blowing snow observational measurements (such as in the suggested regions for lead emissions measurements) and more modeling sensitivity studies. Finally, up to 50% of leads may not be captured in the AMSR-E satellite-derive lead area product as compared to the MODIS product, while leads covered by thin ice, which would not lead to emissions, are included. The net effect of these uncertainties could either lead to an underestimate or overestimate of lead SSA emissions in this study. This satellite

https://doi.org/10.5194/egusphere-2024-3147
Preprint. Discussion started: 17 October 2024

data also covers a past time period (2002-2011), which is not necessarily representative of current conditions, so the location and relative importance of lead emissions could have changed.

Overall, we predict sea ice leads may impact Arctic-wide cold-season SSA concentrations and Br concentrations by up to 5-10% on average during the 2002-2008 period. As leads are likely to increase in prevalence under climate change, including this source of SSA in chemistry and climate models will become more important for future predictions.

Author Contribution

EJE was responsible for data curation, model simulations, validation, visualization, and analysis with expert advice from HMH. HMH is responsible for conceptualization. EJE drafted the manuscript which was revised by HMH.

Competing Interests

The authors declare that they have no conflict of interest.

Acknowledgements

We thank Kerri Pratt for helpful discussions. HMH was supported by Department of Energy (DOE) Atmospheric Systems Research (ASR), award DE-SC0023049. We acknowledge financial support from the department of Civil and Environmental Engineering at the University of Illinois Urbana-Champaign.

Supplemental Information

Equations of SSA flux from Jaegle et a. (2011) and Nilsson et al. (2001); Additional figures of lead SSA emissions for months other than January during the cold season; Cold season total lead SSA emissions; Description and figure of the correlation between lead area and lead SSA emissions; long-term trends in lead area (2002-2011) and relevant statistical testing; additional figures of multi-year (2002-2008) mean percent increase due to leads in SSA and bromine concentration for months other than January during the cold season; Description and figures of correlation between lead emissions and coarse and accumulation mode SSA concentration; Sensitivity simulations.

5. References

https://doi.org/10.5194/egusphere-2024-3147
Preprint. Discussion started: 17 October 2024

553 Abbatt, J. P. D., Thomas, J. L., Abrahamsson, K., Boxe, C., Granfors, A., Jones, A. E., King, M. D., Saiz-Lopez,
554 A., Shepson, P. B., Sodeau, J., Toohey, D. W., Toubin, C., Von Glasow, R., Wren, S. N., and Yang, X.: Halogen
555 activation via interactions with environmental ice and snow in the polar lower troposphere and other
556 regions, Atmospheric Chem. Phys., 12, 6237–6271, https://doi.org/10.5194/acp-12-6237-2012, 2012.

557 Alvarez-Aviles, L., Simpson, W. R., Douglas, T. A., Sturm, M., Perovich, D., and Domine, F.: Frost flower
558 chemical composition during growth and its implications for aerosol production and bromine activation,
559 J. Geophys. Res. Atmospheres, 113, 2008JD010277, https://doi.org/10.1029/2008JD010277, 2008.

560 Amos, H. M., Jacob, D. J., Holmes, C. D., Fisher, J. A., Wang, Q., Yantosca, R. M., Corbitt, E. S., Galarneau,
561 E., Rutter, A. P., Gustin, M. S., Steffen, A., Schauer, J. J., Graydon, J. A., Louis, V. L. St., Talbot, R. W.,
562 Edgerton, E. S., Zhang, Y., and Sunderland, E. M.: Gas-particle partitioning of atmospheric Hg(II) and its
563 effect on global mercury deposition, Atmospheric Chem. Phys., 12, 591–603,
564 https://doi.org/10.5194/acp-12-591-2012, 2012.

565 Chen, Q., Mirrielees, J. A., Thanekar, S., Loeb, N. A., Kirpes, R. M., Upchurch, L. M., Barget, A. J., Lata, N.
566 N., Raso, A. R. W., McNamara, S. M., China, S., Quinn, P. K., Ault, A. P., Kennedy, A., Shepson, P. B.,
567 Fuentes, J. D., and Pratt, K. A.: Atmospheric particle abundance and sea salt aerosol observations in the
568 springtime Arctic: a focus on blowing snow and leads, Atmospheric Chem. Phys., 22, 15263–15285,
569 https://doi.org/10.5194/acp-22-15263-2022, 2022.

570 Community, T. I. G.-C. U.: geoschem/GCClassic: GEOS-Chem 13.2.1, ,
571 https://doi.org/10.5281/ZENODO.5500717, 2021.

572 Confer, K. L., Jaeglé, L., Liston, G. E., Sharma, S., Nandan, V., Yackel, J., Ewert, M., and Horowitz, H. M.:
573 Impact of Changing Arctic Sea Ice Extent, Sea Ice Age, and Snow Depth on Sea Salt Aerosol From Blowing
574 Snow and the Open Ocean for 1980–2017, J. Geophys. Res. Atmospheres, 128, e2022JD037667,
575 https://doi.org/10.1029/2022JD037667, 2023.

576 Cox, C. J., Walden, V. P., Rowe, P. M., and Shupe, M. D.: Humidity trends imply increased sensitivity to
577 clouds in a warming Arctic, Nat. Commun., 6, 10117, https://doi.org/10.1038/ncomms10117, 2015.

578 DeMott, P. J., Hill, T. C. J., McCluskey, C. S., Prather, K. A., Collins, D. B., Sullivan, R. C., Ruppel, M. J.,
579 Mason, R. H., Irish, V. E., Lee, T., Hwang, C. Y., Rhee, T. S., Snider, J. R., McMeeking, G. R., Dhaniyala, S.,
580 Lewis, E. R., Wentzell, J. J. B., Abbatt, J., Lee, C., Sultana, C. M., Ault, A. P., Axson, J. L., Diaz Martinez, M.,
581 Venero, I., Santos-Figueroa, G., Stokes, M. D., Deane, G. B., Mayol-Bracero, O. L., Grassian, V. H., Bertram,
582 T. H., Bertram, A. K., Moffett, B. F., and Franc, G. D.: Sea spray aerosol as a unique source of ice
583 nucleating particles, Proc. Natl. Acad. Sci., 113, 5797–5803, https://doi.org/10.1073/pnas.1514034112,
584 2016.

585 Dibb, J. E., Ziemba, L. D., Luxford, J., and Beckman, P.: Bromide and other ions in the snow, firn air, and
586 atmospheric boundary layer at Summit during GSHOX, Atmospheric Chem. Phys., 10, 9931–9942,
587 https://doi.org/10.5194/acp-10-9931-2010, 2010.

588 Freud, E., Krejci, R., Tunved, P., Leaitch, R., Nguyen, Q. T., Massling, A., Skov, H., and Barrie, L.: Pan-Arctic
589 aerosol number size distributions: seasonality and transport patterns, Atmospheric Chem. Phys., 17,
590 8101–8128, https://doi.org/10.5194/acp-17-8101-2017, 2017.

https://doi.org/10.5194/egusphere-2024-3147
Preprint. Discussion started: 17 October 2024

Gelaro, R., McCarty, W., Suárez, M. J., Todling, R., Molod, A., Takacs, L., Randles, C. A., Darmenov, A., Bosilovich, M. G., Reichle, R., Wargan, K., Coy, L., Cullather, R., Draper, C., Akella, S., Buchard, V., Conaty, A., Da Silva, A. M., Gu, W., Kim, G.-K., Koster, R., Lucchesi, R., Merkova, D., Nielsen, J. E., Partyka, G., Pawson, S., Putman, W., Rienecker, M., Schubert, S. D., Sienkiewicz, M., and Zhao, B.: The Modern-Era Retrospective Analysis for Research and Applications, Version 2 (MERRA-2), J. Clim., 30, 5419–5454, https://doi.org/10.1175/JCLI-D-16-0758.1, 2017.

Gong, S. L.: A parameterization of sea-salt aerosol source function for sub- and super-micron particles, Glob. Biogeochem. Cycles, 17, 2003GB002079, https://doi.org/10.1029/2003GB002079, 2003.

Held, A., Brooks, I. M., Leck, C., and Tjernström, M.: On the potential contribution of open lead particle emissions to the central Arctic aerosol concentration, Atmospheric Chem. Phys., 11, 3093–3105, https://doi.org/10.5194/acp-11-3093-2011, 2011.

Hoffman, J. P., Ackerman, S. A., Liu, Y., and Key, J. R.: A 20-Year Climatology of Sea Ice Leads Detected in Infrared Satellite Imagery Using a Convolutional Neural Network, Remote Sens., 14, 5763, https://doi.org/10.3390/rs14225763, 2022.

Huang, J. and Jaeglé, L.: Wintertime enhancements of sea salt aerosol in polar regions consistent with a sea ice source from blowing snow, Atmospheric Chem. Phys., 17, 3699–3712, https://doi.org/10.5194/acp-17-3699-2017, 2017.

Huang, J., Jaeglé, L., and Shah, V.: Using CALIOP to constrain blowing snow emissions of sea salt aerosols over Arctic and Antarctic sea ice, Atmospheric Chem. Phys., 18, 16253–16269, https://doi.org/10.5194/acp-18-16253-2018, 2018.

Huang, J., Jaeglé, L., Chen, Q., Alexander, B., Sherwen, T., Evans, M. J., Theys, N., and Choi, S.: Evaluating the impact of blowing-snow sea salt aerosol on springtime BrO and O₃ in the Arctic, Atmospheric Chem. Phys., 20, 7335–7358, https://doi.org/10.5194/acp-20-7335-2020, 2020.

Integrated Climate Data Center (ICDC), CEN, and University of Hamburg, Hamburg, Germany: AMSR-E Arctic lead area fraction, n.d.

Intergovernmental Panel On Climate Change: Climate Change 2021 – The Physical Science Basis: Working Group I Contribution to the Sixth Assessment Report of the Intergovernmental Panel on Climate Change, 1st ed., Cambridge University Press, https://doi.org/10.1017/9781009157896, 2023.

Ioannidis, E., Law, K. S., Raut, J.-C., Marelle, L., Onishi, T., Kirpes, R. M., Upchurch, L., Massling, A., Skov, H., Quinn, P. K., and Pratt, K. A.: Modelling wintertime Arctic Haze and sea-spray aerosols, Aerosols/Atmospheric Modelling and Data Analysis/Troposphere/Chemistry (chemical composition and reactions), https://doi.org/10.5194/egusphere-2022-310, 2022.

Jaeglé, L., Quinn, P. K., Bates, T. S., Alexander, B., and Lin, J.-T.: Global distribution of sea salt aerosols: new constraints from in situ and remote sensing observations, Atmospheric Chem. Phys., 11, 3137–3157, https://doi.org/10.5194/acp-11-3137-2011, 2011.

Keller, C. A., Long, M. S., Yantosca, R. M., Da Silva, A. M., Pawson, S., and Jacob, D. J.: HEMCO v1.0: a versatile, ESMF-compliant component for calculating emissions in atmospheric models, Geosci. Model Dev., 7, 1409–1417, https://doi.org/10.5194/gmd-7-1409-2014, 2014.

https://doi.org/10.5194/egusphere-2024-3147
Preprint. Discussion started: 17 October 2024

Kirpes, R. M., Bonanno, D., May, N. W., Fraund, M., Barget, A. J., Moffet, R. C., Ault, A. P., and Pratt, K. A.: Wintertime Arctic Sea Spray Aerosol Composition Controlled by Sea Ice Lead Microbiology, ACS Cent. Sci., 5, 1760–1767, https://doi.org/10.1021/acscentsci.9b00541, 2019.

Leaitch, W. R., Russell, L. M., Liu, J., Kolonjari, F., Toom, D., Huang, L., Sharma, S., Chivulescu, A., Veber, D., and Zhang, W.: Organic functional groups in the submicron aerosol at 82.5° N, 62.5° W from 2012 to 2014, Atmospheric Chem. Phys., 18, 3269–3287, https://doi.org/10.5194/acp-18-3269-2018, 2018.

Li, M., Liu, J., Qu, M., Zhang, Z., and Liang, X.: An Analysis of Arctic Sea Ice Leads Retrieved from AMSR-E/AMSR2, Remote Sens., 14, 969, https://doi.org/10.3390/rs14040969, 2022.

Lin, H., Jacob, D. J., Lundgren, E. W., Sulprizio, M. P., Keller, C. A., Fritz, T. M., Eastham, S. D., Emmons, L. K., Campbell, P. C., Baker, B., Saylor, R. D., and Montuoro, R.: Harmonized Emissions Component (HEMCO) 3.0 as a versatile emissions component for atmospheric models: application in the GEOS-Chem, NASA GEOS, WRF-GC, CESM2, NOAA GEFS-Aerosol, and NOAA UFS models, Geosci. Model Dev., 14, 5487–5506, https://doi.org/10.5194/gmd-14-5487-2021, 2021.

Liu, H., Jacob, D. J., Bey, I., and Yantosca, R. M.: Constraints from ^{210}Pb and ^{7}Be on wet deposition and transport in a global three-dimensional chemical tracer model driven by assimilated meteorological fields, J. Geophys. Res. Atmospheres, 106, 12109–12128, https://doi.org/10.1029/2000JD900839, 2001.

Luo, G. and Yu, F.: Impact of Air Refreshing and Cloud Ice Uptake Limitations on Vertical Profiles and Wet Depositions of Nitrate, Ammonium, and Sulfate, Geophys. Res. Lett., 50, e2023GL104258, https://doi.org/10.1029/2023GL104258, 2023.

Luo, G., Yu, F., and Moch, J. M.: Further improvement of wet process treatments in GEOS-Chem v12.6.0: impact on global distributions of aerosols and aerosol precursors, Geosci. Model Dev., 13, 2879–2903, https://doi.org/10.5194/gmd-13-2879-2020, 2020.

May, N. W., Quinn, P. K., McNamara, S. M., and Pratt, K. A.: Multiyear study of the dependence of sea salt aerosol on wind speed and sea ice conditions in the coastal Arctic, J. Geophys. Res. Atmospheres, 121, 9208–9219, https://doi.org/10.1002/2016JD025273, 2016.

Monahan, E. C., Spiel, D. E., and Davidson, K. L.: A Model of Marine Aerosol Generation Via Whitecaps and Wave Disruption, in: Oceanic Whitecaps, vol. 2, edited by: Monahan, E. C. and Niocaill, G. M., Springer Netherlands, Dordrecht, 167–174, https://doi.org/10.1007/978-94-009-4668-2_16, 1986.

Nilsson, E. D., Rannik, Ü., Swietlicki, E., Leck, C., Aalto, P. P., Zhou, J., and Norman, M.: Turbulent aerosol fluxes over the Arctic Ocean: 2. Wind-driven sources from the sea, J. Geophys. Res. Atmospheres, 106, 32139–32154, https://doi.org/10.1029/2000JD900747, 2001.

Pierce, J. R. and Adams, P. J.: Global evaluation of CCN formation by direct emission of sea salt and growth of ultrafine sea salt, J. Geophys. Res. Atmospheres, 111, 2005JD006186, https://doi.org/10.1029/2005JD006186, 2006.

Pound, R. J., Sherwen, T., Helmig, D., Carpenter, L. J., and Evans, M. J.: Influences of oceanic ozone deposition on tropospheric photochemistry, Atmospheric Chem. Phys., 20, 4227–4239, https://doi.org/10.5194/acp-20-4227-2020, 2020.

https://doi.org/10.5194/egusphere-2024-3147
Preprint. Discussion started: 17 October 2024

Pratt, K. A., Custard, K. D., Shepson, P. B., Douglas, T. A., Pöhler, D., General, S., Zielcke, J., Simpson, W. R., Platt, U., Tanner, D. J., Gregory Huey, L., Carlsen, M., and Stirm, B. H.: Photochemical production of molecular bromine in Arctic surface snowpacks, Nat. Geosci., 6, 351–356, https://doi.org/10.1038/ngeo1779, 2013.

Quinn, P. K., Coffman, D. J., Kapustin, V. N., Bates, T. S., and Covert, D. S.: Aerosol optical properties in the marine boundary layer during the First Aerosol Characterization Experiment (ACE 1) and the underlying chemical and physical aerosol properties, J. Geophys. Res., 103, 16,547-16,563, 1998.

Quinn, P. K., Bates, T. S., Miller, T. L., Coffman, D. J., Johnson, J. E., Harris, J. M., Ogren, J. A., Forbes, G., Anderson, T. L., Covert, D. S., and Rood, M. J.: Surface submicron aerosol chemical composition: What fraction is not sulfate?, J. Geophys. Res. Atmospheres, 105, 6785–6805, https://doi.org/10.1029/1999JD901034, 2000.

Quinn, P. K., Miller, T. L., Bates, T. S., Ogren, J. A., Andrews, E., and Shaw, G. E.: A 3-year record of simultaneously measured aerosol chemical and optical properties at Barrow, Alaska, J. Geophys. Res. Atmospheres, 107, https://doi.org/10.1029/2001JD001248, 2002.

Radke, L. F., Hobbs, P. V., and Pinnons, J. E.: Observations of Cloud Condensation Nuclei, Sodium-Containing Particles, Ice Nuclei and the Light-Scattering Coefficient Near Barrow, Alaska, J. Appl. Meteor. Climatol., 15, 982–995, https://doi.org/10.1175/1520-0450(1976)015%3C0982:OOCCNS%3E2.0.CO;2, 1976.

Reiser, F., Willmes, S., and Heinemann, G.: A New Algorithm for Daily Sea Ice Lead Identification in the Arctic and Antarctic Winter from Thermal-Infrared Satellite Imagery, Remote Sens., 12, 1957, https://doi.org/10.3390/rs12121957, 2020.

Rhodes, R. H., Yang, X., Wolff, E. W., McConnell, J. R., and Frey, M. M.: Sea ice as a source of sea salt aerosol to Greenland ice cores: a model-based study, Atmospheric Chem. Phys., 17, 9417–9433, https://doi.org/10.5194/acp-17-9417-2017, 2017.

Riley, J. P. and Chester, R.: Introduction to marine chemistry, Academic Press, London, New York, 465 pp., 1971.

Röhrs, J. and Kaleschke, L.: An algorithm to detect sea ice leads by using AMSR-E passive microwave imagery, The Cryosphere, 6, 343–352, https://doi.org/10.5194/tc-6-343-2012, 2012.

Roscoe, H. K., Brooks, B., Jackson, A. V., Smith, M. H., Walker, S. J., Obbard, R. W., and Wolff, E. W.: Frost flowers in the laboratory: Growth, characteristics, aerosol, and the underlying sea ice, J. Geophys. Res., 116, D12301, https://doi.org/10.1029/2010JD015144, 2011.

Schmale, J., Zieger, P., and Ekman, A. M. L.: Aerosols in current and future Arctic climate, Nat. Clim. Change, 11, 95–105, https://doi.org/10.1038/s41558-020-00969-5, 2021.

Scott, W. D. and Levin, Z.: Open Channels in Sea Ice (Leads) as Ion Sources, Science, 177, 425–426, https://doi.org/10.1126/science.177.4047.425, 1972.

https://doi.org/10.5194/egusphere-2024-3147
Preprint. Discussion started: 17 October 2024

Simpson, W. R., Alvarez-Aviles, L., Douglas, T. A., Sturm, M., and Domine, F.: Halogens in the coastal snow pack near Barrow, Alaska: Evidence for active bromine air-snow chemistry during springtime, Geophys. Res. Lett., 32, 2004GL021748, https://doi.org/10.1029/2004GL021748, 2005.

Simpson, W. R., Von Glasow, R., Riedel, K., Anderson, P., Ariya, P., Bottenheim, J., Burrows, J., Carpenter, L. J., Frieß, U., Goodsite, M. E., Heard, D., Hutterli, M., Jacobi, H.-W., Kaleschke, L., Neff, B., Plane, J., Platt, U., Richter, A., Roscoe, H., Sander, R., Shepson, P., Sodeau, J., Steffen, A., Wagner, T., and Wolff, E.: Halogens and their role in polar boundary-layer ozone depletion, Atmospheric Chem. Phys., 7, 4375–4418, https://doi.org/10.5194/acp-7-4375-2007, 2007.

Stramler, K., Del Genio, A. D., and Rossow, W. B.: Synoptically Driven Arctic Winter States, J. Clim., 24, 1747–1762, https://doi.org/10.1175/2010JCLI3817.1, 2011.

Stutz, J., Thomas, J. L., Hurlock, S. C., Schneider, M., Von Glasow, R., Piot, M., Gorham, K., Burkhart, J. F., Ziemba, L., Dibb, J. E., and Lefer, B. L.: Longpath DOAS observations of surface BrO at Summit, Greenland, Atmospheric Chem. Phys., 11, 9899–9910, https://doi.org/10.5194/acp-11-9899-2011, 2011.

Sumata, H., De Steur, L., Divine, D. V., Granskog, M. A., and Gerland, S.: Regime shift in Arctic Ocean sea ice thickness, Nature, 615, 443–449, https://doi.org/10.1038/s41586-022-05686-x, 2023.

Swanson, W. F., Holmes, C. D., Simpson, W. R., Confer, K., Marelle, L., Thomas, J. L., Jaeglé, L., Alexander, B., Zhai, S., Chen, Q., Wang, X., and Sherwen, T.: Comparison of model and ground observations finds snowpack and blowing snow aerosols both contribute to Arctic tropospheric reactive bromine, Atmospheric Chem. Phys., 22, 14467–14488, https://doi.org/10.5194/acp-22-14467-2022, 2022.

Vaughan, D., Comiso, J., Allison, I., Carrasco, J., Kaser, G., Kwok, R., Mote, P., Murray, T., Paul, F., Ren, J. F., Rignot, E., Solomina, O., Steffen, K., and Zhang, T.: Observations: Cryosphere, in: Climate Change 2013: The Physical Science Basis, 317–382, 2013.

Wang, Q., Jacob, D. J., Spackman, J. R., Perring, A. E., Schwarz, J. P., Moteki, N., Marais, E. A., Ge, C., Wang, J., and Barrett, S. R. H.: Global budget and radiative forcing of black carbon aerosol: Constraints from pole-to-pole (HIPPO) observations across the Pacific, J. Geophys. Res. Atmospheres, 119, 195–206, https://doi.org/10.1002/2013JD020824, 2014.

Wang, Q., Danilov, S., Jung, T., Kaleschke, L., and Wernecke, A.: Sea ice leads in the Arctic Ocean: Model assessment, interannual variability and trends, Geophys. Res. Lett., 43, 7019–7027, https://doi.org/10.1002/2016GL068696, 2016.

Wang, X., Jacob, D. J., Downs, W., Zhai, S., Zhu, L., Shah, V., Holmes, C. D., Sherwen, T., Alexander, B., Evans, M. J., Eastham, S. D., Neuman, J. A., Veres, P. R., Koenig, T. K., Volkamer, R., Huey, L. G., Bannan, T. J., Percival, C. J., Lee, B. H., and Thornton, J. A.: Global tropospheric halogen (Cl, Br, I) chemistry and its impact on oxidants, Atmospheric Chem. Phys., 21, 13973–13996, https://doi.org/10.5194/acp-21-13973-2021, 2021.

Wang, Y., Jacob, D. J., and Logan, J. A.: Global simulation of tropospheric O_3-NO_x-hydrocarbon chemistry: 3. Origin of tropospheric ozone and effects of nonmethane hydrocarbons, J. Geophys. Res. Atmospheres, 103, 10757–10767, https://doi.org/10.1029/98JD00156, 1998.

https://doi.org/10.5194/egusphere-2024-3147
Preprint. Discussion started: 17 October 2024

738 Willis, M. D., Leaitch, W. R., and Abbatt, J. P. D.: Processes Controlling the Composition and Abundance of
739 Arctic Aerosol, Rev. Geophys., 56, 621–671, https://doi.org/10.1029/2018RG000602, 2018.

740 World Meteorological Organization (WMO): WMO/GAW aerosol measurement procedures, guidelines
741 and recommendations, WMO, Geneva, 2003.

742 Yang, X., Neděla, V., Runštuk, J., Ondrušková, G., Krausko, J., Vetráková, Ľ., and Heger, D.: Evaporating
743 brine from frost flowers with electron microscopy and implications for atmospheric chemistry and sea-
744 salt aerosol formation, Atmospheric Chem. Phys., 17, 6291–6303, https://doi.org/10.5194/acp-17-6291-
745 2017, 2017.

746 Zhang, L., Gong, S., Padro, J., and Barrie, L.: A size-segregated particle dry deposition scheme for an
747 atmospheric aerosol module, Atmos. Environ., 35, 549–560, 2001.

748